J Mater Sci (2011) 46:6075–6086
DOI 10.1007/s10853-011-5570-0

Morphological, thermal, rheological, and mechanical properties of polypropylene-nanoclay composites prepared from masterbatch in a twin screw extruder

Achmad Chafidz · Mohammad Al-haj Ali · Rabeh Elleithy

Received: 22 February 2011 / Accepted: 16 April 2011 / Published online: 3 May 2011

Abstract A commercial homopolymer polypropylene was melt blended with commercial nanoclay masterbatch at different concentrations of nanoclay using twin screw extruder (TSE). The influence of three different concentrations (5, 10, and 15 wt%) of the nanoclay on the morphological, thermal, rheological, and mechanical properties was investigated. The morphology of the nanocomposites was characterized using Scanning Electron Microscope (SEM), whereas, the thermal behavior (e.g., melting and crystallization) was characterized using Differential Scanning Calorimetry (DSC). The melt rheology and dynamic mechanical properties were analyzed using a torsional rheometer. Additionally, the tensile properties were characterized as well. The morphological analysis showed that the nanoclay was well distributed in the PP matrix as indicated by the SEM micrographs. The DSC results showed that the presence of nanoclay in the PP matrix increased the degree of crystallinity of PP-nanoclay composites, which reached a maximum at 5 wt% of nanoclay concentration. However, the melting temperature of the PP-nanoclay composites was not affected by the presence of nanoclay particles. In addition, rheological analysis showed that the melt response gradually changed from pseudo-liquid like to pseudo-solid like as the nanoclay concentration increased. Moreover, the storage modulus (G') increased by increasing nanoclay content. Furthermore, tensile test results showed that the addition of nanoclay leads to a significant enhancement in the mechanical properties of the PP nanocomposites.

A. Chafidz · M. A. Ali
Department of Chemical Engineering, King Saud University, Riyadh, Saudi Arabia

R. Elleithy (✉)
SABIC Polymer Research Center, King Saud University, Riyadh, Saudi Arabia
e-mail: rhelleithy@yahoo.com

Introduction

Reinforcement of polymers using fillers is generally carried out in the production of high performance plastics. It has been many years since the manufacturer has filled polymer with particles/fillers (polymer composites) in order to enhance the properties of polymer materials. However, although conventionally filled polymeric materials are vastly used, generally this addition of fillers sometimes causes disadvantages to the resulting composite materials like brittleness, because there is no or only little interaction at the interface between the two mixed components. Generally, macro-sized reinforcing fillers usually give imperfections especially in the resulted material's structure, which also affects other properties like ductility and toughness [1–3].

A radical alternative to the conventional polymer composites is provided by polymer nanocomposites (PNCs), a promising new class of composite materials. PNCs consist of a polymeric material (e.g., thermoplastics, thermosets, or elastomers) and a reinforcing nano-sized material (nanomaterial). The dispersed nanomaterial has at least one dimension in nanometer scale. Because the nanomaterials are so small, limited amounts are sufficient to greatly enhance the polymer properties. Thus, the use of such materials has no effect on polymer density and processability compared to their traditional composites. This feature counterbalanced the negative effect of high cost of nanofillers [1, 3, 4].

The unique characteristic of polymer nanocomposites is caused by the fundamental nanoscale dimensions which

dominate the morphology and properties of polymer nanocomposites material. The uniform dispersion of nano-sized particles (nanofillers e.g., nanoclays, nanofibers, nanotubes) can lead to an extremely large interfacial area and even high aspect ratio (largest dimension/smallest dimensions of nanofiller). Thus, increasing the interaction between polymer matrix and nanofiller leads to properties enhancement of polymer nanocomposites [4–6]. Polymer nanocomposites offer the possibility to develop new materials with their own different-structure property relationships compared to the micron and macro scale composites. Polymer nanocomposites (PNCs) exhibit improved tensile strength and moduli [1, 5], improved thermal degradation [7], decreased gas permeability [8, 9], and reduced flammability [10–13].

Among the potential nanomaterials used in polymer nanocomposites, nanoclay (layered silicate) has been widely investigated primarily because of remarkable improvement in properties. Furthermore, clay materials are easily available, environmentally friendly, and their intercalation chemistry has been investigated for a long time. These make nanoclay one of the most widely accepted and effective nano-reinforcements [1, 4, 14–16].

Several methods have been considered to prepare polymer—layered silicate nanocomposites, exfoliation—adsorption, in situ intercalative polymerization, template synthesis, and direct melt intercalation using a polymer mixer or extruder. For the development of most important polymer, both in situ polymerization and exfoliation—adsorption is limited because neither a suitable monomer nor a compatible polymer—silicate system is always available. Moreover, they are not always compatible with current polymer processing techniques. The remaining option that has attracted great interest among researchers and thus particularly will be used in this study is melt intercalation method. This method is compatible with current industrial processes as extrusion and injection molding. Besides, it is environmental friendly because no solvent is used. Using melt intercalation, suitable nanoclay can be blended with PP to produce nanocomposites [1, 17–19]. Nanoclay is a hydrophilic material, whereas PP is one of the most hydrophobic polymers. This fact makes nanoclay difficult to exfoliate or intercalate in the polypropylene matrix. In order to render its surface more hydrophobic which improves the compatibility with PP, surface treatment of nanoclay (organoclay) is necessary [4, 17, 19, 20].

PP-nanoclay composites have been widely investigated by numerous researchers [3, 4, 15–18, 20–24]. Recently, commercial nano-material masterbatches have been already manufactured. Using commercial masterbatch becomes a promising alternative in the production of polymer nanocomposites compared with using bulk nanomaterials. Besides dust free, masterbatch also has less healthy and safety risks. Another advantage of masterbatch is the elimination of difficulty in dispersion process and also easy handling because the nano-materials are bounded inside the polymer matrix. Therefore, the use of masterbatch in producing polymer nanocomposites is considered to be one of the simplest and most economical methods in processing of polymer-nanocomposites. However, literature survey revealed that the investigation reports which studied polypropylene nanocomposites using masterbatch are limited compared to direct incorporation of nanomaterial into polypropylene that makes it an attractive area for research [25].

The aim of this study is to evaluate the effectiveness of nanoclay concentration, added as a masterbatch, on morphological, thermal, rheological, and mechanical properties of PP-nanoclay composites. This study demonstrated the successful preparation of PP nanoclay composites using commercial masterbatch.

Experimental

Materials

Commercial homopolymer polypropylene was used as matrix polymer for the nanocomposites which were investigated in this study. The polypropylene was acquired from a local manufacturer in the Saudi market. Table 1 shows some properties of the polypropylene according to the manufacturer's datasheet. As for the nano-filler, commercial nanoclay masterbatch materials, *NanoMax*, with 50 wt% concentration of nanoclay and PP as carrier were supplied by Nanocor, USA. According to the product information from the supplier, the nanoclay is organophillic montmorillonite (MMT), which has been modified with dimethyl-dihydrogenated tallow ammonium and it is believed that the masterbatch contains maleic anhydride (MA) as a compatibilizer.

Table 1 Some properties of polypropylene homopolymer according to the manufacturer

Property	Unit	Value	Test method
Melt flow rate (2.16 kg and 230 °C)	g/10 min	8	ASTM D-1238
Tensile strength at yield	MPa	32	ASTM D-638
Tensile elongation at yield	%	11	ASTM D-638
Flexural modulus (1% secant)	MPa	1630	ASTM D-256
Heat distortion temperature	°C	100	ASTM D-648
Vicat softening temperature	°C	155	ASTM D-1525B

Preparation of PP-nanoclay composites

PP-nanoclay composites (PPNCs) were prepared by diluting highly concentrated nanoclay masterbatch pellets in polypropylene matrix using melt blending technique. First, polypropylene was manually pre-mixed with different concentration of masterbatch (10, 20, and 30 wt%), which effectively is 5,10, and 15 wt% of nanoclay. Prior to the melt blending in a twin screw extruder (TSE), the mixed materials (PP and nanoclay masterbatch) were dried in an conventional oven at 55 °C for 24 h to reduce the moisture content. It is known that high moisture content inside the blend/mixture could produce bubbles during the processing step.

Afterward, the pre-mix was compounded using co-rotating twin screw extruder, Farrell FTX-20. The screw diameter is 26 mm and the L/D ratio 35. The TSE has distributive and dispersive mixing elements. The extrudate from the die was cooled in water bath (at about 20 °C), air dried, and pelletized for further use. Details about the processing conditions of TSE are listed in Table 2. The nanocomposite samples will be referred to as NC-5, NC-10, NC-15 for nanoclay concentration of 5, 10, and 15 wt%, respectively. The same extrusion procedure was used on neat PP (referred to as NC-0) to compare pure material with its nanocomposites.

The prepared pellets from TSE were dried as mentioned before, then were further used to make a set of molded samples for testing. An injection molding machine, Super Master Series SM 120, made by Asian Plastic Machinery Co. was used to prepare a set of ASTM standard samples (e.g., tensile and flexural). The injection molding conditions are listed in Table 3.

Note that we used different masterbatch concentrations in this study; *some of them could be seen as high concentrations*, to investigate the optimum concentration of nanoclay. We tried to balance the gained benefits of using the masterbatch with the added cost that comes with them.

Samples characterization

Morphological analysis

Scanning electron microscopy (SEM) images were obtained using a JEOL JSM-6360A, Japan. Molded samples were cryogenically fractured in order to maintain the originality of the sample's morphology. Afterward, the fractured samples were coated with a thin layer of gold (good conductive metal) in order to minimize samples electronic charging and overheating. In addition, the coating can also increase the signal and surface resolution. All the samples were examined by the SEM at 15 kV using different magnifications that vary from 200 to 20,000×.

Table 2 Processing conditions of twin screw extruder (TSE)

Barrel temp. (°C)		Screw speed (rpm)	Melt press. (bar)
Zone 1	Zone 2–6		
230	240	17	12

Thermal analysis

A differential scanning calorimeter (DSC), model DSC-60 from Shimadzu—Japan, was used to study the melting and crystallization behavior of the nanocomposites. DSC temperature scale was calibrated from the melting characteristics of indium. Nanocomposite samples of about 5–7 mg each were accurately weighted and then analyzed via DSC. The samples were heated at constant rate of 10 °C/min from ambient temperature up to 200 °C (approx. 30 °C higher than the melting temperature of PP) in air environment. They were held for 5 min at 200 °C to erase their thermal history. Subsequently, samples were cooled down to 30 °C at a cooling rate of 10 °C/min to study the crystallization process. Finally, samples were heated again for the second time (2nd heating scan) at a constant rate of 10 °C/min up to 350 °C. The corresponding thermograms were recorded. All DSC curves were normalized to the unit weight of the sample.

The melting temperature, T_m was taken as the peak temperature of the transition endothermic curve from the 2nd heating scan whereas, the crystallization temperature, $T_{c,}$ was taken as the peak temperature of the transition exothermic curve during the cooling scan. The crystallinity of the specimen was calculated from the experimental heat of fusion ΔH_m and the literature value of 100% crystalline polymer material, ΔH_m^0. Literature indicates that ΔH_m^0 for PP is 207 J/g [26]. The following equation was used to estimate the percentage of crystallinity (X_c) [27]:

$$X_c = \frac{\Delta H_m}{\Delta H_m^0} \cdot 100[\%] \quad (1)$$

Rheological/viscoelastic characterization

The melt rheological measurements were performed using a Rheometer instrument model AR G2 made by TA Instruments, USA. The complex viscosity of neat PP and its nanocomposites were measured under torsion mode using frequency sweep scheme in parallel plates fixture with diameter equal to 25 mm and a constant 2 mm gap. Stress sweep tests were also performed on representative samples to determine their linear viscoelastic region. Prior, frequency sweep tests were performed at a constant temperature, of 260 °C. Oscillation stress was kept constant at

Table 3 Processing conditions of injection molding machine

Screw speed (rpm)	Temperature (°C)				Injection pressure (bar)	Cooling time (s)	Cycle time (s)
200	T 1	T 2	T 3	Feed zone	500	30	35
	220	240	240	170			

500 Pa. This value is within the range of linear viscoelastic region of each nanocomposites, which was determined based on the oscillation stress vs. % (shear) strain curve generated from stress sweep test. The data generated from this frequency sweep test were storage modulus (G'), loss modulus (G''), and complex viscosity (η^*) versus angular frequency in frequency range between 0.1 and 628.3 rad/s. Disk-like samples with diameter 25 mm and thickness approximately 3 mm obtained from injection molding were used for this test. Excess of polymer melts were cleaned prior to the test.

Dynamic mechanical analysis (DMA) was performed to characterize the viscoelastic behavior of the solid material at different temperatures. DMA was carried out by using the same apparatus, Rheometer-AR G2. The analysis was carried under torsion mode using temperature sweep scheme. The angular frequency was 1 rad/s, and the strain was 1%. This strain was in the linear viscoelasticity region of PP and the nanoclay composites. The temperature sweep was between 30 and 140 °C with 3 °C increment. Rectangular samples, with dimensions of 3.25 mm thick × 12.70 mm width × 63.5 mm length obtained from injection molding machine were used for this test.

Mechanical properties

Tensile tests were performed on dumbbell-shape tensile bars (tensile sample prepared by injection molding machine) by using LYOD tensile test machine at room temperature and a cross-head speed of 500 mm/min. ASTM D-638 was used as our guidelines. Displacement was measured from the cross-head position. The stress–strain curves and the mechanical properties e.g., estimated tensile modulus (E), maximum stress, tensile energy to break (or toughness), and strain at break were calculated. The values were taken from the median of three runs for each of nanocomposites.

Results and discussion

Morphology

Scanning electron micrographs of cryo-fractured surface of PP-nanoclay composite samples at different concentration (5 and 15 wt%) are presented in Fig. 1. The study of the SEM micrographs revealed that all the samples show good distribution of nanoclay particles. Nanoclay is indicated by the white needle-like nanoclay in dark area of the PP matrix. Even at high nanoclay concentration (15 wt%), the distribution of nanoclay particles in PP matrix was still good. Relatively small size of the nanoclay particles are scattered uniformly in PP matrix (Fig. 1d). This good distribution of nanoclay could be attributed to the high shear stress that the polymer melt was exposed to during processing which was induced by the twin screw geometry and temperature in the barrel. Uniform distribution is an important aspect that needs to be considered because if the resulted nanocomposites consist of aggregates of nanoclay particles, the stress in the aggregate's area will be high, resulting in crack initiation and propagation, and consequent premature failure [16].

Using a commercial software, Sigma Scan (Systat Software Inc. from US), SEM images (Fig. 1) were further analyzed. In this study, we performed the distribution of particles area. Figure 2a and b show the distribution of nanoclay particles area of NC-5 and NC-15 nanocomposite samples, respectively. The distribution of particles area on this SEM image analysis only covered nanoclay particles with area approximately $\geq$0.3 μm^2. Smaller particles were not analyzed here due to the limitations of the SEM apparatus.

In addition, both of NC-5 and NC-15 nanocomposite samples showed comparative trend of nanoparticles area distribution. However, NC-15 had some particles bigger than 3 μm^2. As noticed in both Fig. 2a and b, the highest population number of nanoclay particles had an area less or equal to 1 μm^2. This means that the well distribution or even dispersion of nanoclay particles in PP matrix was considerably assisted by intercalants. Therefore, surface modification for nanoclay is a very crucial aspect to improve the affinity or compatibility between nanoclay and the polymer matrix and to avoid the agglomeration [4]. Several research studies on PLS nanocomposites have shown a significant change in the viscoelastic property depending on their microstructure and the interfacial characteristics between polymer and layered silicate (intercalation or exfoliation) [22, 27, 28].

Both of SEM image analyses (NC-5 and NC-15) revealed that the area of nanoclay in PP matrix was far below 5% of total area of SEM image. Thus, it could be assumed that the "undetected nanoclay particles" were in nanometer scale, which can only be observed using different microscopic techniques such as TEM.

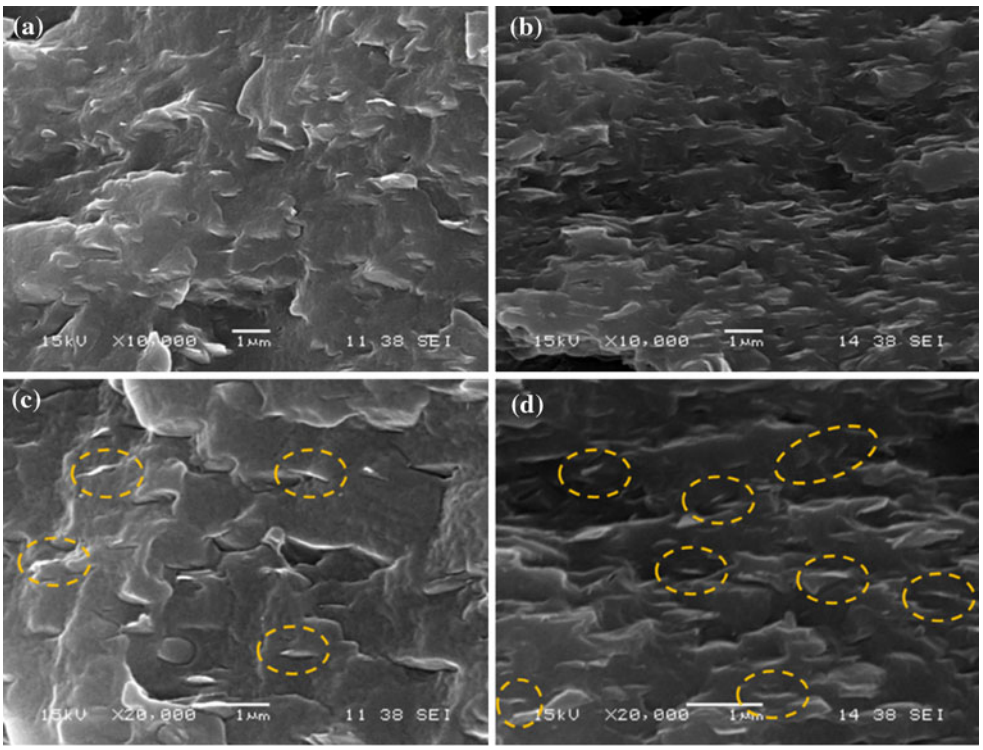

Fig. 1 SEM images of NC-5 (*left*) and NC-15 (*right*) at different magnification, **a** and **b** (10,000×); **c** and **d** (20,000×). *Dashed circles* show some of nanoclay particles

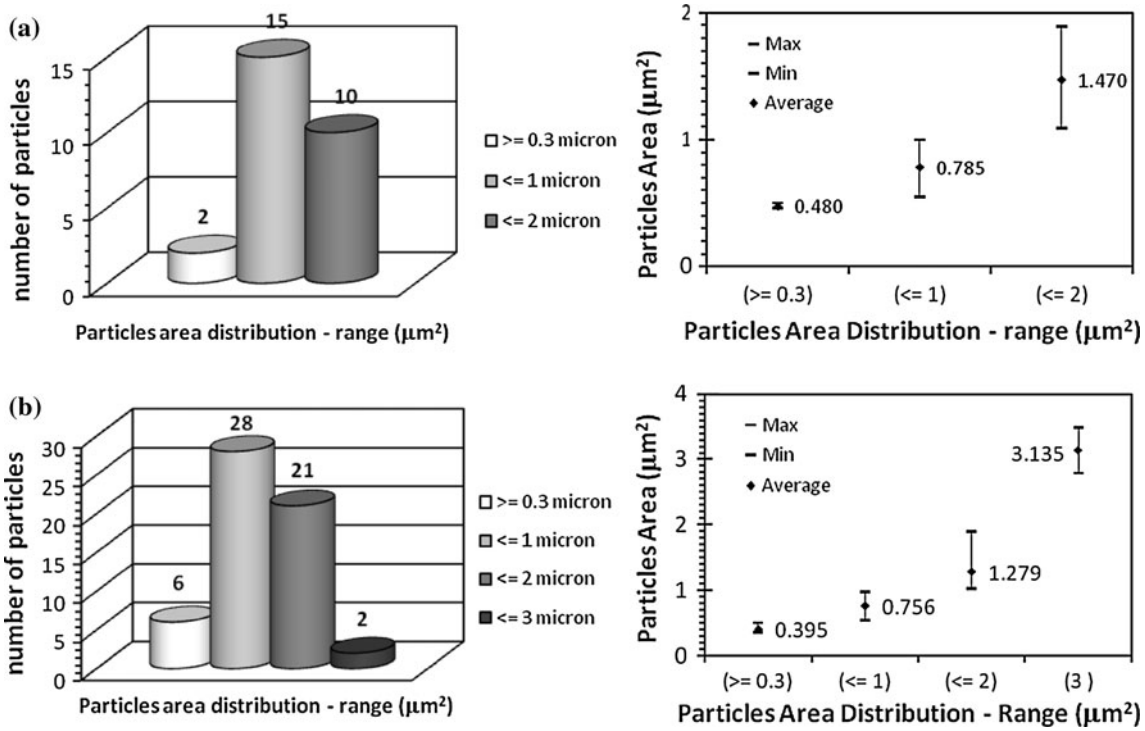

Fig. 2 **a** Distribution of nanoclay particles area in NC-5 nanocomposite sample (scan image analysis result of Fig. 1**c**). **b** Distribution of nanoclay particles area in NC-15 nanocomposite sample (scan image analysis result of Fig. 1**d**)

Thermal behavior (non-isothermal crystallization)

Figure 3 shows the DSC melting curves of PP-nanoclay composites prepared using twin screw extruder. The transition DSC melting curves were chosen from the 2nd heating scan to eliminate the influence from the thermo mechanical history of the samples. The thermal analysis results in terms of melting temperature (T_m), heat of fusion (ΔH), and the percentage of crystallinity (X_c) were determined from the thermograms (Fig. 3) and are summarized in Table 4.

The DSC measurement showed that the melting temperatures of PP-nanoclay composites were not significantly affected by the changes in the nanoclay concentration. Similar result was also observed by Zhou et al. [29]. In addition, the degree of crystallinity, X_c of PP-nanoclay composites slightly increased as compared to that of neat PP as shown in Table 4. The increase of X_c could be attributed to the presence of the dispersed nanoclay platelets, which enhanced the nucleation process of PP by acting as heterogeneous nuclei during the crystallization process [23]. However, X_c reached a maximum of 51.2% at 5 wt% nanoclay concentration. Thereafter, X_c decreased at higher concentrations (15 wt%) (Fig. 3 and Table 4). The decrease of X_c could be explained by the presence of an excessive number of nanoclay platelets which could hinder the motion of the polymer chain segments and thus, retard crystal growth [30]. There are two mutually opposite effects of nanoclay on the crystallization behavior; nucleating ability and growth retardation. Both of them are related to the type, content, and dispersion state of the nanoclay [15]. The combination of a large amount of nucleation sites and limited crystal growth is expected to produce crystal of fine grain size. It is inferred that the addition of organoclay increased the number and decreased the size of spherulites formed in polypropylene. Similar case was reported by Ma et al. [31] and Xu et al. [32].

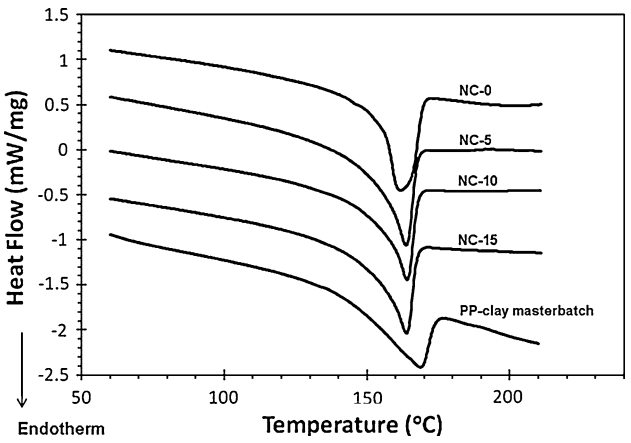

Fig. 3 DSC melting curves (2nd heating scan) of PP-nanoclay composites. The *curves* have been shifted in the *y*-direction to make them distinguishable

To investigate the effect of different nanoclay concentrations on the crystallization behavior, DSC cooling curves of different mixtures of PP-nanoclay composites are shown in Fig. 4. Crystallization temperature (T_c), and the T onset crystallization (T_{oc}) were determined from the thermograms and summarized in Table 4. As noticed from the figure, crystallization process of PP-nanoclay composite for all nanoclay concentrations has two peaks as compared to the neat PP which has a single crystallization peak. In this study, it is suggested that the first crystallization peak at lower temperature, Tc_1, was attributed to the homogeneous crystallization of neat PP. The second crystallization peak at higher temperature, Tc_2, was attributed to the crystallization process induced by the heterogeneous nucleation resulting from the presence of nanoclay, that was confirmed by comparing the crystallization peak (T_c) of the nanoclay masterbatch to that of neat PP. The nanoclay masterbatch had T_c of 126 °C close to T_{c_2}, as compared to neat PP which had T_c of 113 °C, close to T_{c_1}.

The presence of nanoclays in the mixtures increased the crystallization temperature, T_c significantly, from 113 °C (PP) to approximately 126 °C. It indicates that the presence of nanoclay altered the overall crystallization process of PP matrix by acting as nucleating agent. Many research studies have shown a nucleating effect of nanoclay particles [4, 31, 33]. Lei et al. reported that the presence of nanoclays in the PP-nanoclay composites increased the T_c from 107 °C (PP) to about 115 °C [4].

The contribution of heterogeneous and homogeneous portion in overall crystallization process could be estimated by comparing the area of each peak (heterogeneous and homogeneous). Using commercial software, "Peak Fit" made by Systat Software Inc.-USA, each exothermic curve was deconvoluted/separated into two peaks which represent heterogeneous and homogeneous crystallization peaks, and then the area of each peak was calculated. The results in the form of a percentage of each area can be seen in Table 5. As shown in Table 5, by adding nanoclay, heterogeneous crystallization mechanism took over the crystallization process. This phenomenon could be seen clearly in Fig. 5, as noticed, the nanoclay acted effectively as nucleating agent. Note that for PP-nanoclay masterbatch, concentration was 50 wt%. In addition, the ratio of hetero- to homo-crystallization was almost independent of the nanoclay percentage used here. This topic is currently under further investigation.

Moreover, from Table 4 another advantage of nanoclay addition into PP matrix could be derived. As noticed, there was a significant difference in the onset crystallization temperature, T_{oc} where T_{oc} of PP-nanoclay composites experienced a shift to higher temperatures with difference

Table 4 DSC results for PP-nanoclay composites prepared by using TSE machine

Sample	T_m (°C) ±0.2%	Heat of fusion (J/g) ±2%	X_c (%) ±2%	Tc_1 (°C) ±0.2%	Tc_2 (°C) ±0.2%	T onset crystallization, T_{oc} (°C) ±0.2%
NC-0	162	98	47.3	113	–	117
NC-5	164	106	51.2	114	126	130
NC-10	164	102	49.3	114	126	130
NC-15	164	91	44.0	114	126	130
PP-nanoclay masterbatch	168	68	32.9	–	126	132

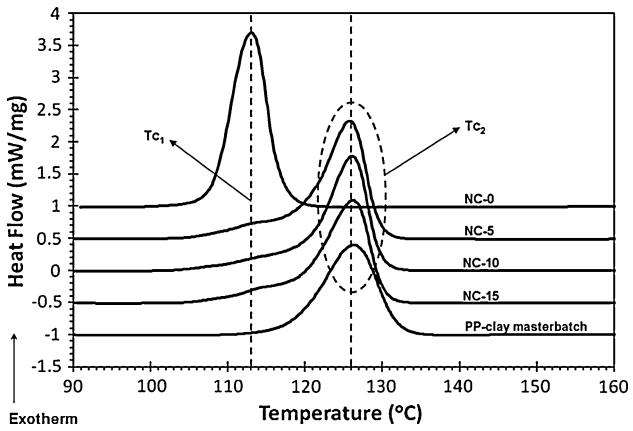

Fig. 4 DSC crystallization (cooling) curves of PP-nanoclay composites (TSE I) at a cooling rate of −10 °C/min. The *curves* have been shifted in the *y*-direction to make them distinguishable

Table 5 Comparison of homogenous and heterogeneous crystallization process based on deconvolution method

Sample	Crystallization mechanism (%)	
	Homogeneous	Heterogeneous
NC-0	100	0
NC-5	16	84
NC-10	16	84
NC-15	14	86
PP-nanoclay masterbatch	0	100

of about 13 °C compared with neat PP. This will be a great advantage in the injection molding process because the solidification of the molded parts would start earlier; this shortens the molding cycle, which means an economic advantage.

Melt rheological properties

Shown in Fig. 6 are the results of the frequency sweep tests that were performed. As the frequency increased, the storage modulus (G') and loss modulus (G'') of PP-nanoclay composites also increased. It is noticed from the figure that melt rheological behavior of PP significantly changed

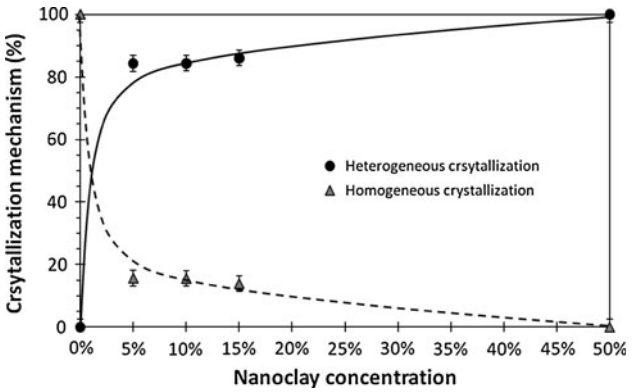

Fig. 5 Comparison of homogenous and heterogeneous crystallization process of PP-nanoclay composites based on deconvolution method

after nanoclay incorporation into PP matrix. At lower frequencies region ($\omega < 10$ rad/s), the melt rheological behavior (e.g., the slope) of nanocomposites was very different from that of the neat PP especially at higher nanoclay concentration (10 and 15 wt%). Both G' and G'' for the nanocomposites exhibited diminished frequency dependence. While, at lower nanoclay concentration (5 wt%), the melt rheological behavior looked similar to that of neat PP. This indicates that the viscoelastic properties are still dominated by the polymer matrix. On the other hand, at higher frequencies region ($\omega > 10$ rad/s), melt rheological behavior (e.g., the slope) of PP-nanoclay composites looked similar. It was not affected by the addition of nanoclay particles, because it was merely dominated by the motion of short chains [34].

The possible explanation for this phenomenon was proposed by Ren et al. [35], who conducted stress relaxation measurements to understand the viscoelastic behavior observed at low frequencies region for the nanocomposites. The authors suggested that such behavior is due to the presence of stacked intercalated silicate layers, which are randomly oriented in the polymer matrix, forming three dimension networking structure. These layers have only translational motion. A high amplitude oscillatory shear orients these structures and reduces the pseudo solid-like behavior. Another explanation is the physical jamming of the dispersed stack intercalated silicate layers, because of their highly anisotropic nature [36].

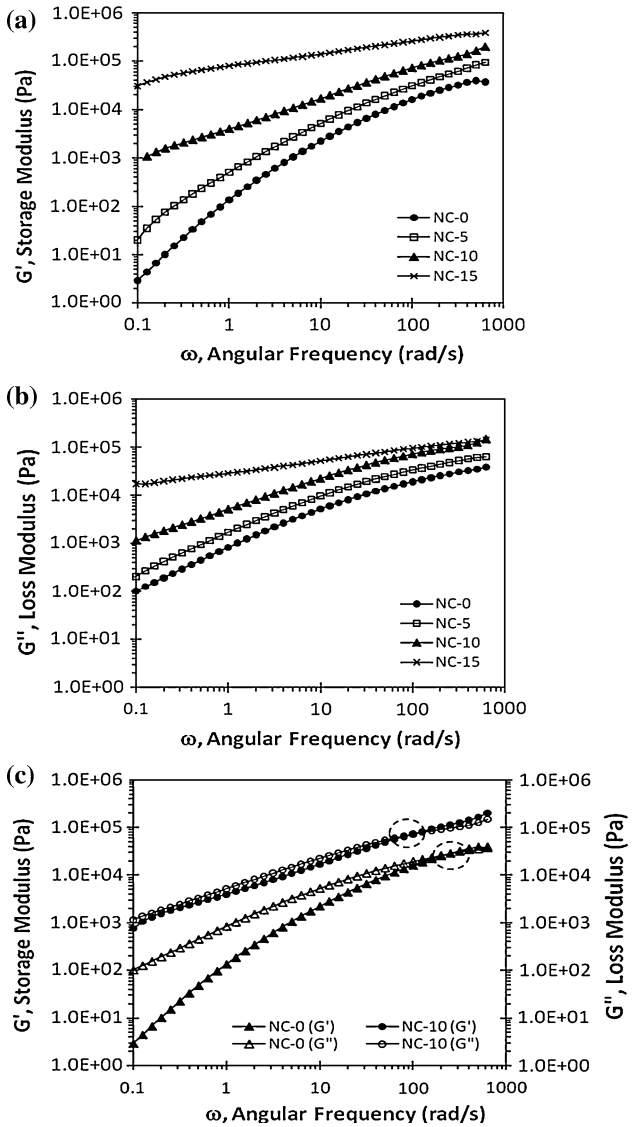

Fig. 6 Storage modulus (**a**) and loss modulus (**b**) versus angular frequency, and (**c**) cross-over points of PP-nanoclay composites at temperature 260 °C

In addition, at lower frequencies region ($\omega < 10$ rad/s), as nanoclay concentration in the PP matrix increased, viscoelastic response of the nanocomposites gradually changed from pseudo-liquid like ($G' < G''$) to pseudo-solid like ($G' > G''$). In fact, for PP-nanoclay composites with highest nanoclay concentration (NC-15), G' was not very sensitive to the increase of angular frequency at lower frequencies region as compared to the neat PP. The G' of NC-15 exceeded its G'' at frequency lower than 0.1 rad/s; which means that characteristic of the material exhibiting a pseudo-solid like behavior. Similar results have been observed by Koo et al. [22]. It is suggested that the polymer chains could not relax completely, due to the interaction between polymer and nanoclay. Interfacial characteristics between nanoclay particles and polymer matrix as well as the microstructural difference gave a strong relationship between morphological and rheological properties, which manifested in the change of the viscoelastic properties [22, 27, 28, 37].

If Figs. 6a and b (storage and loss modulus) were overlapped, there will be an intersection between the two moduli. The storage modulus gradually exceeded the loss modulus, which indicated a shift from pseudo liquid-like behavior to pseudo solid-like behavior. Along with the increasing of nanoclay concentration, there was a trend, where the intersection shifts toward lower frequency. The intersections were at 251.2, 158.5, and 100 rad/s for PP, NC-5, and NC-10, respectively while at NC-15, the intersection is at lower frequency, outside the boundary of our range of the test. In addition, Fig. 6a shows that G' of neat PP increased about 10,000 times from 0.1 to 100 rad/s, whereas G' of NC-15 increased only about 10 times for the same frequency range. This could be attributed to the molecular mobility that was restricted for NC-15 while it was not for neat PP.

Figure 7 shows the effect of nanoclay concentration on the dynamic complex viscosity $|\eta^*|$ of nanoclay composites. From the figure, it is noticed that the dynamic complex viscosity increased substantially with increased nanoclay content. This increase was attributed to the interaction and dispersion of nanoclay in the polymer matrix that appeared to provide the flow restriction of polymer chain in the molten state. In addition, at lower frequency region ($\omega < 1$ rad/s), neat PP exhibit some Newtonian-like behavior indicated by the plateau régime. As the nanoclay concentration increased, the Newtonian-like behavior dependency diminished. The Newtonian plateau is an indication of the cooperative interaction of the molecules. As the interaction increased, the plateau "length" decreased. For the NC-15, the nanoclay helped the interaction between the molecules; hence the plateau ended at lower frequency and got shortened. In addition, all nanoclay composites exhibited an increased shear thinning behavior, which is attributed to the orientation of the nanoclay layers under shear. Similar result was also reported by Kim et al. [21]; Sinha Ray and Okamoto [38] and Koo et al. [22].

Dynamic mechanical properties

The effect of nanoclay concentration on the temperature dependencies of the dynamic storage modulus, G' which is analogous to the stiffness of neat PP and PP-nanoclay composites is presented in Fig. 8. As noticed from Fig. 8, the storage moduli of nanocomposites are higher when compared with that of neat PP. The storage modulus of the samples increased by adding the nanoclay, which resulted in a considerable improvement in stiffness. This phenomenon could be attributed to the restricted mobility of PP

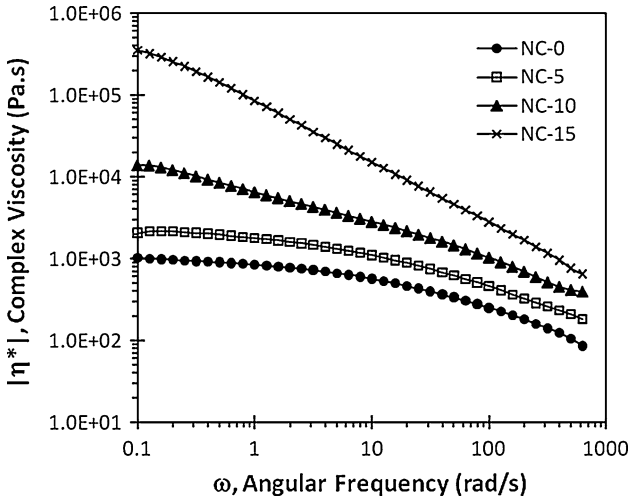

Fig. 7 Dynamic complex viscosity $|\eta^*|$ as function of angular frequency (ω) for PP-nanoclay composites at 260 °C

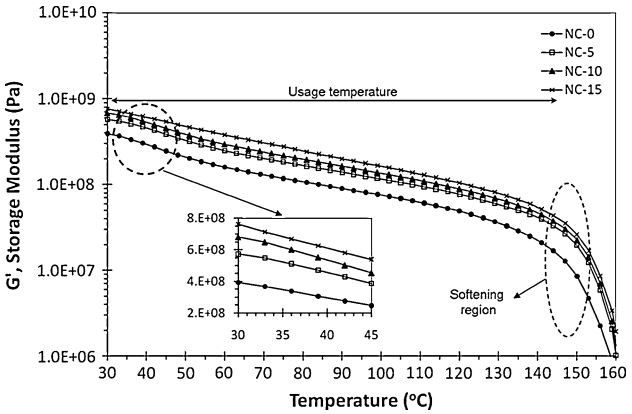

Fig. 8 Temperature dependencies of storage modulus (G') of PP-nanoclay composites at angular frequency 1 rad/s and constant 0.1% strain

chains as a result of the interaction between nanoclay and PP matrix. There are several factors that affect this interaction; however, this interaction strongly depends on the interfacial area shared between PP and the nanoclay. As the concentration of nanoclay increased, the interaction area also increased. This explains the improvement of the storage modulus of the nanocomposites by increasing the level of the nanoclay concentrations [22, 39].

Figure 8 shows that all curves have the same trend, which is the sharp decrease of the storage modulus at higher temperatures. This is due to the molecular mobility which is less restricted at high temperature [20]. The curves in Fig. 8 could be divided into two regions; flat region and steep region. The flat region determines the "usage temperatures" of each material. From these curves, the "softening temperatures" could also be determined and are listed in Table 6. The "softening temperature" is defined as the temperature where the storage modulus starts to decline sharply, which is taken as the intersection of the flat and steep regions tangents. The softening temperature is considered as the maximum usage temperature of the material. As noticed from Table 6, the "softening temperature" of the nanocomposites was relatively higher than that of the neat PP. Hence, the addition of nanoclay widened the usage-temperature range of the nanocomposites as compared to neat PP.

To get more insight into the effect of nanoclay in enhancing the stiffness of PP material, the representative values of the storage modulus of PP-nanoclay composites TSE I at temperature of 30, 60, 100, and 130 °C are listed in Table 6. For example, at 100 °C, there are improvements in storage modulus values of nanocomposite samples as compared to the neat PP. The increasing of storage modulus (stiffness) of PP-nanoclay composites as compared to neat PP are about 56, 82, and 121% for 5, 10, and 15 wt% of nanoclay concentration, respectively.

Such significant enhancements look interesting from industrial applications point of view. As an example, let us assume that the design criterion for a certain part dictates a minimum modulus of 160 MPa. By using neat PP, this limit value is reached at 60 °C while using nanocomposites material the limit is reached at higher temperature of 100 °C. This 40 °C temperature difference shows that the incorporation of nanoclay particles into PP matrix greatly enhanced the thermal stability of the matrix and hence widened its "usage temperature".

The relationship between storage modulus, percentage of nanoclay concentration (%), and temperature (T) was modeled using the following exponential equation, Eq. 2.

Table 6 The representative values of storage modulus, G' at several temperatures for PP-nanoclay composites prepared using TSE

Sample	G' (Pa) at temperature				Softening
	30 °C	60 °C	100 °C	130 °C	Temperature (°C)
NC-0	3.9E + 08	1.6E + 08	7.7E + 07	3.7E + 07	145
NC-5	5.7E + 08	2.5E + 08	1.2E + 08	6.1E + 07	149
NC-10	6.8E + 08	2.9E + 08	1.4E + 08	7.0E + 07	150
NC-15	7.6E + 08	3.8E + 08	1.7E + 08	8.2E + 07	151

$$G' = Ae^{B(T)} \quad (2)$$

where G' is storage modulus as a function of nanoclay loading in wt%, the type of nanoclay, and temperature. Parameters A and B are to be determined from the fitting of the experimental data, which is presented in Table 6. It is worth mentioning that the fitting data were only applied for "the flat region" or usage temperature (30–130 °C). Our model showed that parameter A (MPa) was a function of the concentration of the nanoclay as described by Eq. 3.

$$A = 4.91E7 * (\text{wt}\%) + 7.47E8 \quad (3)$$

Parameter B ($1/K$) was found to be independent of the nanoclay concentration; for the nanocomposite studied in this study, it has a value of -0.0221. This parameter is expected to change if different nanoclay is used. Eq. 2 described the nanocomposites satisfactorily; however, it did not model the neat PP very well.

In order to clarify the significant effect of nanoclay addition in enhancing PP properties, the relative storage modulus of PP-nanoclay composites to those of PP are plotted in Fig. 9. The relative storage moduli of PP-nanoclay composites were higher than those of the respective PP matrix at all temperature range. As could be seen in the figure, the relative storage modulus of PP-nanoclay composites increased as nanoclay concentration increased

In addition, the storage modulus of NC-15 (15 wt% of nanoclay) considerably increased up to the peak tops at approximately 50–70 °C and then slightly decreased, as described as hump-like curve. This "peak" could be attributed to the development of nanoclay network that resisted the applied stress. This network resistance increased as the concentration of nanoclay increased as shown by the size of the peak. For example, the peak of NC-15 was bigger than that of NC-5. As the temperature increased, mobility of the network increased and the network structure collapsed causing the modulus to decrease. Similar result was also observed by Hasegawa, et al. [40]. They found that relative storage modulus of PP-nanoclay hybrids (PPCHs) drastically increased up to the peak tops at about 60–70 °C and then decreased. In general, the improvements of the storage modulus were about 1.5–2.2 fold times as compared to that of neat PP. Similar results were also observed in several research investigations [4, 18, 40, 41].

Moreover, the relative storage moduli of all nanocomposites were gradually increased; starting at 120 °C and reached the top peak at 155 °C as indicated by hump-like curves. This "peak" phenomenon could be related to the DSC melting curves. As seen in the Fig. 3, melting process for all samples started at about 120 °C and completely melted at about 164 °C. Apparently, the "peak" phenomenon has emerged in this range of temperature. As nanoclay concentration increased, the "peak" tendency becomes bigger and bigger. It is suggested that the structure of nanocomposites during the melting process was different than that of neat PP. The structure changes as nanoclay concentration increased. The presence of nanoclay particles hindered the motion of polymer chains, resulted in different storage modulus response than that of neat PP. However, this phenomenon needs further investigation.

Mechanical properties

Figure 10 shows the results of tensile stress–strain curve as function of nanoclay concentration level. As shown in this figure, there was an increase in tensile modulus, E, and yield stress. As the concentration of nanoclay increased, so did the tensile modulus. This improvement could be seen in Table 7, which shows some of mechanical properties (e.g., tensile modulus, yield stress, toughness, and strain at

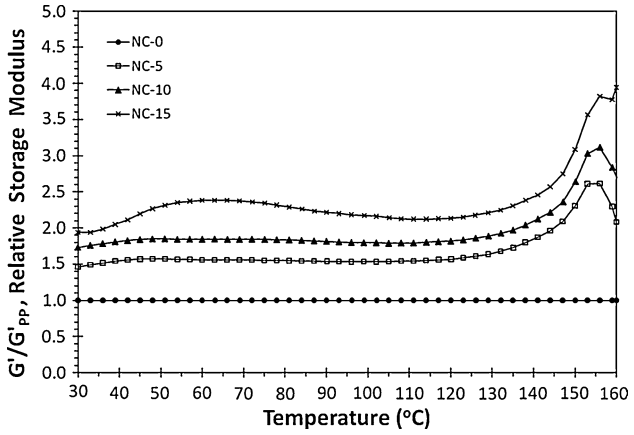

Fig. 9 Temperature dependencies of relative storage modulus (G') of PP-nanoclay composites as compared to neat PP at angular frequency 1 rad/s

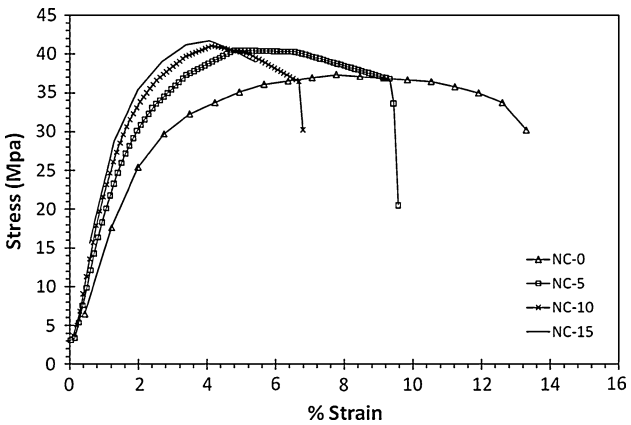

Fig. 10 Stress–strain curves of neat PP and its nanocomposites at cross-head speed of 500 mm/min

Table 7 Mechanical properties of neat PP and PP-nanoclay composites at different nanoclay concentration

Sample	Tensile modulus, E (MPa)	Yield stress (MPa)	Strain at break (%)	Toughness (MJ/m^3)
NC-0	1560	37.4	13.1	4.0
NC-5	2154	41.0	9.6	2.7
NC-10	2330	41.1	6.8	1.8
NC-15	2787	41.8	5.4	1.3

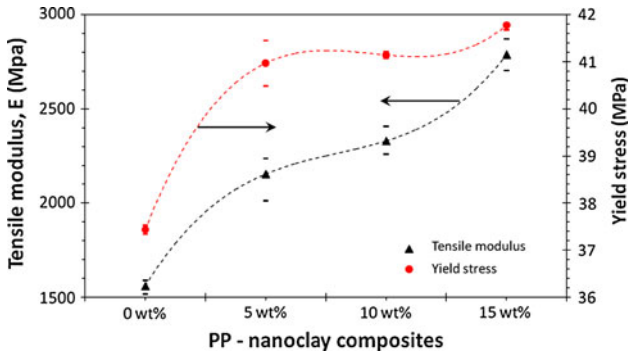

Fig. 11 Modulus elasticity, E, and yield stress of PP-nanoclay composites with different nanoclay concentration at cross-head speed of 500 mm/min

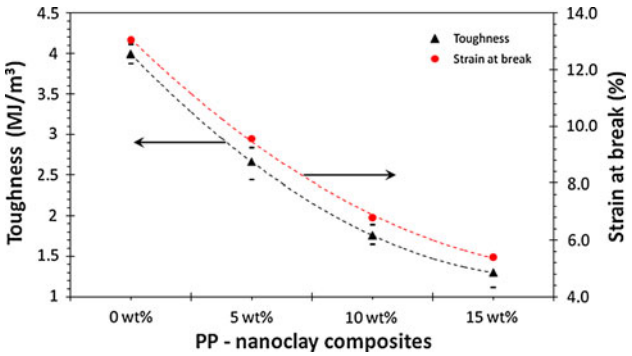

Fig. 12 Toughness and ultimate strain of PP-nanoclay composites with different nanoclay concentration at cross-head speed of 500 mm/min

break) that generated from Fig. 10. The data were taken as mean of three runs. The tensile modulus increased by 38, 49, and 79% on the addition of nanoclay at 5, 10, and 15 wt%, respectively (see Fig. 11).

The increasing of tensile modulus, E, is analogous to the increasing of storage modulus, G', due to the restricted motion of the polymer chains, which resulted from the strong interaction between the PP matrix and nanoclay [21, 22]. Tensile modulus enhancements were also reported in other research investigation with different use of polymer matrix [21, 38, 41]. Another important tensile property is the yield stress. The yield stress (here taken as the peak stress) of nanoclay composites are presented in Fig. 11. From the figure, we can see that the yield stress of PP material has been enhanced by the incorporation of nanoclay in PP matrix. However, as noticed in Table 6, the toughness of PP-nanoclay composites decreased as nanoclay concentration increased. This could be explained by the presence of the nanoclay which could act as a stress concentrator that will decrease the toughness of the composites. Toughness was more sensitive to strain rather than the yield stress. Figure 12 shows the toughness and strain at break (ultimate strain) of the nanocomposites as function of nanoclay concentration. As noticed from the figure, the toughness and strain at break (ultimate strain) decreased about 67 and 60%, respectively (for NC-15) as compared to that of neat PP. It is an indication of a less mobility of the polymer chains caused by interaction between PP matrix and nanoclay particles.

Conclusions

Melt-blended PP-nanoclay composites with different nanoclay concentration were successfully prepared from commercial masterbatch. The effect of nanoclay concentration on morphological, thermal, rheological, and mechanical properties of the prepared nanocomposites has been studied. These results suggested that the optimum loading is 5%. Morphological study revealed that all the samples showed good distribution and dispersion of nanoclay particles in PP matrix at all concentrations. This could be attributed to the high shear stressed of the polymer melt during processing and surface modification of nanoclay particles. Thus, using masterbatch yielded good distribution of nanoclay in the composite. DSC results revealed that introducing nanoclay particles in PP matrix enhanced the degree of crystallinity at certain nanoclay concentration, namely 5%. Nanoclay particles acted as nucleating agent, thus promoting heterogeneous crystallization process, and hence enhancing the degree of crystallinity. Two crystallization mechanisms existed which resulted into two crystallization peaks that were attributed to the homogeneous and heterogeneous crystallization temperatures. The nanocomposites experienced a shift to a higher temperature of crystallization, which could be translated as money savings in polymer processing like injection molding process. In rheological behavior, the nanocomposites showed higher storage modulus, loss modulus, and complex viscosity than the neat PP. Evidence of changes from pseudo-liquid like ($G' < G''$) to

pseudo-solid like ($G' > G''$) appeared as the nanoclay concentration increased which showed an intense relationship with their morphologies. Dynamic mechanical analysis (DMA) results showed that the addition of nanoclay into PP matrix resulted in a significant improvement of storage modulus of the nanocomposites; the increase was proportional to the concentration of the nanoclay. The improvements of the storage modulus of the nanocomposites at 30 °C were 1.5–2.2 fold times as compared to that of neat PP. The reinforced effect in storage modulus by incorporating nanoclay was most effective, especially in the higher temperature range rather that the lower temperature ranges. It was also found that the addition of nanoclay increased the thermal stability of the nanocomposites, which makes it possible to use PP-nanoclay composites at higher temperature than the neat PP. Mechanical test results showed that the addition of nanoclay in PP matrix leads to a significant enhancement in the stiffness of PNC, while the yield stress was only enhanced at certain level, and further loading of the nanoclay had less effect on the yield stress. In contrary, the toughness of PP-nanoclay composites decreased as nanoclay concentration increased.

Acknowledgements The authors are grateful to SABIC Polymer Research Center (SPRC) at King Saud University for allowing us to use their equipments and to the Engineering Research Center for their financial support. We would also like to thank the Deanship of Scientific Research and Research Center-College of Engineering at King Saud University.

References

1. Alexandre M, Dubois P (2000) Mater Sci Eng 28(1–2):1
2. Fischer H (2003) Mater Sci Eng 23(6–8):763
3. Modesti M, Lorenzetti A, Bon D, Besco S (2005) Polymer 46(23):10237
4. Lei SG, Hoa SV, Ton-That MT (2006) Compos Sci Technol 66(10):1274
5. Kannan M, Bhagawan SS, Jose T (2010) J Mater Sci 45:1078. doi:10.1007/s10853-009-4046-y
6. Nath DC, Bandyopadhyay S, Yu A, Zeng Q, Das T, Blackburn D, White C (2009) J Mater Sci 44:6078. doi:10.1007/s10973-009-0408-6
7. Ganguly A, Bhowmick A (2009) J Mater Sci 44:903. doi:10.1007/s10853-008-3183-z
8. Yano K, Usuki A, Okada A, Kurauchi T, Kamigaito O (1993) J Polym Sci 31(10):2493
9. Messersmith PB, Giannelis EP (1995) J Polym Sci 33(7):1047
10. Gilman JW, Kashiwagi T, Brown JET, Lomakin SP (1998) In: Proceeding of 43rd international SAMPE symposium and exhibition—materials and process affordability keys to the future, Book1, vol 43, 31 May–4 June 1998, Anaheim, CA
11. Gilman JW (1999) Appl Clay Sci 15(1–2):31
12. Gilman JW, Jackson CL, Morgan AB, Harris R Jr (2000) Chem Mater 12(7):1866
13. Kashiwagi T, Du F, Douglas JF, Karen IW, Harris R Jr, Shields JR (2005) Nat Mater 4(12):928
14. Mai YW, Yu ZZ (2006) Polymer nanocomposites. Woodhead Publishing Ltd., Cambridge
15. Yuan Q, Awate S, Misra RDK (2006) Eur Polym J 42(9):1994
16. Yuan Q, Misra RDK (2006) Polymer 47(12):4421
17. Modesti M, Lorenzetti A, Bon D, Besco S (2006) Polym Degrad Stab 91(4):672
18. Hasegawa N, Kawasumi M, Kato M, Usuki A, Okada A (1998) J Appl Polym Sci 67(1):87
19. Lertwimolnun W, Vergnes B (2005) Polymer 46(10):3462
20. Rohlmann CO, Failla MD, Quinzani LM (2006) Polymer 47(22):7795
21. Kim DH, Fasulo PD, Rodgers WR, Paul DR (2007) Polymer 48(18):5308
22. Koo CM, Kim MJ, Choi MH, Kim SO, Cheung IJ (2003) J Appl Polym Sci 88(6):1526
23. Sharma SK, Nayak SK (2009) Polym Degrad Stab 94(1):132
24. Boucard S, Duchet J, Gerard JF, Prele P, Gonzales S (2003) Macromol Symp 194(1):241
25. Prashantha K, Soulestin J, Lacrampe MF, Krawczak P, Dupin G, Claes M (2008) Compos Sci Technol 69(11–12):1756
26. Ehrenstein GW, Riedel G, Trawiel P (2004) Thermal analysis of plastic: theory and practice. Carl Hanser Verlag, Munich
27. Kim HB, Choi JS, Lee CH, Lim ST, Jhon MS, Choi HJ (2005) Eur Polym J 41(4):679
28. Lim YT, Park OO (2001) Rheol Acta 40(3):220
29. Zhou Y, Rangari V, Mahfuz H, Jeelani S, Mallick PK (2005) Mater Sci Eng 402(1–2):109
30. Kontou E, Niaounakis M (2006) Polymer 47(4):1267
31. Ma J, Zhang S, Qi Z, Li G, Hu Y (2002) J Appl Polym Sci 83(9):1978
32. Xu Y, Shang S, Huang J (2010) Polym Test 29:1007–1013
33. Kodgire P, Kalgaonkar R, Hambir S, Bulakh N, Jog JP (2001) J Appl Polym Sci 81(7):1786
34. Ferry JD (1980) Viscoelastic properties of polymer. Wiley, New York, p 358
35. Ren J, Silva AS, Krishnamoorti R (2000) Macromolecules 33(10):3739
36. Ray SS (2006) J Ind Eng Chem 12(6):811
37. Ray SS, Okamoto M (2003) Prog Polym Sci 28(11):1539
38. Ray SS, Okamoto M (2003) Macromol Mater Eng 288(12):936
39. Nwabunma D, Kyu T (2008) Polyolefin composites. Wiley-Interscience, New Jersey
40. Hasegawa N, Okamoto H, Kato M, Usuki A (2000) J Appl Polym Sci 78(11):1918
41. Kim JH, Koo CM, Choi YS, Wang KH, Chuung IJ (2004) Polymer 45:7719